# Type specification of stability islands and chaotic stickiness

Oded Barash and Itzhack Dana
*Minerva Center and Department of Physics, Bar-Ilan University, Ramat-Gan 52900, Israel*
(Received 16 August 2004; published 28 March 2005)

A detailed characterization of stability islands in area-preserving maps is introduced on the basis of the *resonance partition* of phase space and it is used to define chaotic stickiness in these maps. It is shown that a general island can be characterized by a well-defined quasiregularity "type," specifying the sequence of resonances visited by the island. In particular, a "tangle" island lies entirely not just within the turnstile lobe of a resonance but also within the *turnstile overlap* of two resonances. Chaotic stickiness to a given island is then defined as the coincidence of the type of a chaotic orbit with that of the island in some time interval. This definition allows one to study stickiness systematically on *all* time scales, including short or nonasymptotic time regimes, as illustrated in the case of an accelerator-mode island of the standard map. A physically significant identification of the "sticky layer" and its "sublayers" in this case is made and discussed.

DOI: 10.1103/PhysRevE.71.036222 PACS number(s): 05.45.Ac, 45.05+x, 05.45.Mt

## I. INTRODUCTION

Regular-motion components in generic Hamiltonian systems usually have a strong impact on chaotic dynamics and transport [1–17]. A well-known and significant phenomenon is the "stickiness" of chaotic orbits to the boundaries of stability islands, causing anomalous chaotic transport [1,3,11–17]. Area-preserving maps with an integrable limit feature two distinct kinds of islands [18] (see also Sec. III): (a) resonance islands, lying forever within a given resonance and having a near-integrable limit, and (b) "tangle" islands, lying in the turnstile lobe of a resonance and therefore visiting also the exterior of the resonance. These islands are born by bifurcation and have no near-integrable continuation. An important case of a tangle island is the "accelerator-mode" island (AI), featured by systems having some periodicity in phase space, such as the maps (1) below. Stickiness to the boundaries of AI's can lead to a superdiffusion of the chaotic motion [11–17].

Stickiness is usually conceived as the long-time trapping of chaotic orbits in extremely complex dynamical structures—e.g., islands-around-islands hierarchies [3]—surrounding the boundary of a given island and adjacent to it. It seems then impossible to define stickiness precisely and understand it completely in terms of all these structures. In this paper, we introduce a detailed characterization of stability islands on the basis of the *resonance partition* of phase space [4–10]. We then show that this characterization leads in a natural way to a precise generalized definition of stickiness. This definition allows us to study stickiness systematically on *all* time scales, including short or nonasymptotic time regimes. We shall focus on kicked-rotor maps on the cylinder,

$$M:\ p_{n+1}=p_n+Kf(x_n),\quad x_{n+1}=x_n+p_{n+1} \bmod 2\pi, \tag{1}$$

where $p$ is the angular momentum, $x$ is the angle, $K$ is a nonintegrability parameter, and $f(x+2\pi)=f(x)$. Strong numerical evidence [4,9] and exact results [5,7] indicate that at least for a subclass of maps (1) the rotational resonances, suitably defined (see Sec. II), give a complete partition of phase space in the absence of separating tori; this implies a "quasiregularity" of almost all the orbits, specified by their "type"—i.e., the sequence of resonances visited [8,9] (see a summary in Sec. II). We then show in Sec. III that a general island chain can be characterized by a well-defined type—i.e., the type of its central stable periodic orbit. The statement that a tangle island lies in a turnstile lobe [18] is sharpened: it actually lies entirely within the *turnstile overlap* of two resonances. In Sec. IV, chaotic stickiness is defined as the coincidence of the type of a chaotic orbit with that of a given island chain in some time interval. On the basis of this definition, first aspects of stickiness in a nonasymptotic time regime are studied in detail in the case of an AI of the standard map. A physically significant identification of the "sticky layer" and its "sublayers" in this case is made and discussed in the concluding section (Sec. V).

## II. RESONANCE PARTITION AND ROTATIONAL QUASIREGULARITY

We summarize here the construction of rotational resonances [4] for the standard map [map (1) with $f(x)=\sin(x)$] and the related notion of "quasiregularity" [8,9]. For any rational number $l/m$ ($l$ and $m$ are coprime integers) and for arbitrarily large $K$, the standard map possesses one hyperbolic periodic orbit (PO) having period $m$ ($x_m=x_0,\ p_m=p_0$) and the *order-preserving* (or *monotonicity*) property [7,10,19]; i.e., the relative positions of $x_n$ in $[0,2\pi)$ are the same as those of $x_n=x_n^{(0)}$ in the $K=0$ case of a pure rotation with winding number $l/m$: $x_n^{(0)}=x_0^{(0)}+2\pi nl/m \bmod 2\pi$, $n=0,\ldots,m-1$. A "gap" is a pair of PO points having neighboring values of $x_n \bmod 2\pi$. The gap widths in the $x$ direction are not all equal to $2\pi/m$, as in the $K=0$ case, but due to the order-preserving property, the iterate of a gap is still a gap. One gap, called the "principal" gap, appears to be always symmetrically positioned around the "dominant" symmetry line $x=\pi$—i.e., $\pi-x_L=x_R-\pi$, where $L$ and $R$ denote the left and right points, respectively, of the principal gap. The $l/m$ *resonance* [20] and its *turnstiles* are now defined as follows (see also Figs. 1 and 2). We denote by $\mathcal{Z}^{(0)}(l/m)$ the

 

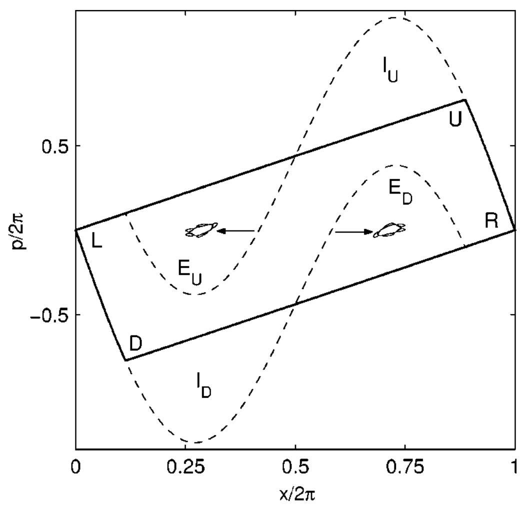


FIG. 1. Region *LURD* (solid lines): principal zone $\mathcal{Z}^{(0)}$ of resonance $l/m=0/1$ of the standard map for $K=6.4717$ (strong-chaos regime). This zone, which is the resonance itself in this $m=1$ case, is bounded by pieces $\overrightarrow{DL}$, $\overrightarrow{LU}$, $\overrightarrow{UR}$, and $\overrightarrow{RD}$ of the stable and unstable manifolds of the hyperbolic fixed point $L$ (or $R$). The upper (lower) turnstile consists of the exiting lobe $E_U$ ($E_D$) and the entering lobe $I_U$ ($I_D$), which is outside the resonance. The arrows indicate period-1 accelerator-mode islands (AI's) surrounded by five-island chains (see more details in Fig. 4). The AI's are clearly tangle islands lying in the exiting lobes $E_U$ and $E_D$.

region *LURD* (see Fig. 1 for the case of $l/m=0/1$), bounded by pieces of the stable and unstable manifolds of $L$ and $R$ under the map $M^m$. Here $U$ ($D$) is a primary homoclinic intersection—i.e., the upper (lower) intersection closest to the line $x=\pi$ from the right (from the left). The $l/m$ resonance is then the chain of $m$ zones $\mathcal{Z}^{(n)}(l/m)=M^{-n}\mathcal{Z}^{(0)}(l/m)$, $n=0,\ldots,m-1$; see Fig. 2. Clearly, the zone $\mathcal{Z}^{(m)}(l/m)=M^{-m}\mathcal{Z}^{(0)}(l/m)$ lies again in the principal gap and

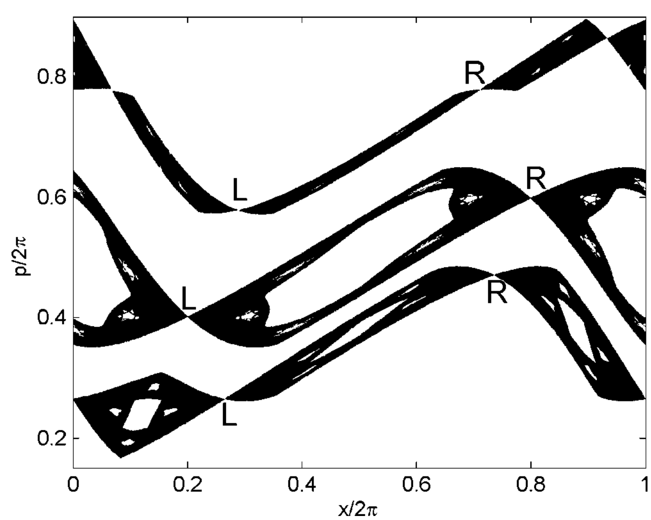


FIG. 2. Chaotic components of resonances 1/3, 1/2, and 3/4 of the standard map for $K=1.3$, calculated using the efficient method introduced in Ref. [9], which avoids the problem of finding the resonance boundaries. The turnstiles (not shown) are always associated with the principal zone in the principal gap *LR*.

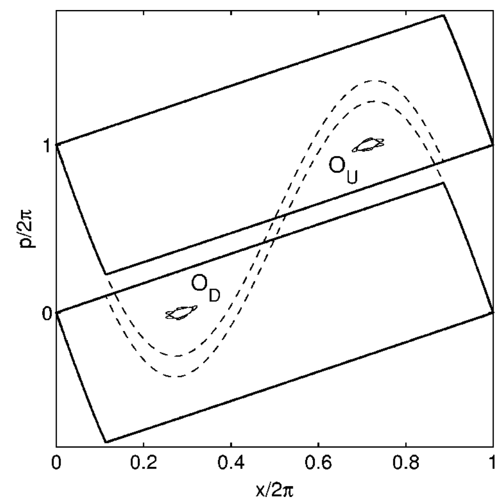


FIG. 3. Resonances 0/1 and 1/1 of the standard map for $K=6.4717$ (compare with Fig. 1). The region $O_D=\mathcal{O}(0/1\rightarrow 1/1)$ $[O_U=\mathcal{O}(1/1\rightarrow 0/1)]$ is the overlap of the exiting lobe of the upper [lower] turnstile of 0/1 [1/1] with the entering lobe of the lower [upper] turnstile of 1/1 [0/1]. The AI's indicated in Fig. 1 are shown also here. Clearly, they lie entirely within $O_D$ and $O_U$.

differs from $\mathcal{Z}^{(0)}(l/m)$ by two turnstiles created by homoclinic oscillations under $M^{-m}$; see Fig. 1. Each turnstile consists of two lobes of equal area. By construction, the lobes outside (inside) $\mathcal{Z}^{(0)}(l/m)$ form the region entering (exiting) resonance $l/m$. Generally, an exiting $l/m$ turnstile lobe overlaps with an entering $l'/m'$ turnstile lobe for $l'/m'$ sufficiently close to $l/m$; see Fig. 3. This *turnstile overlap* (TO) $\mathcal{O}(l/m\rightarrow l'/m')$ is precisely the region in resonance $l/m$ escaping to resonance $l'/m'$ in one iteration.

Strong numerical evidence [4,9] and exact results [5] indicate that in the absence of rotational tori—i.e., for $K>K_c\approx 0.9716$—the resonances constructed as above give a complete *partition* of phase space [21]. This seems to hold also for more general maps possessing some "reversibility" symmetry [4]—e.g., maps (1) with $f(-x)=-f(x)$—and can be rigorously proven for the sawtooth map [with $f(x)=x$ for $-\pi<x<\pi$ and $f(-\pi)=0$] [7] which is a good approximation of the standard map for large $K$. The resonance partition implies that a general orbit (except for a zero-measure set of aperiodic orbits—e.g., cantori) must have all its points within resonances and must therefore perform a quasiregular motion as follows. Suppose that the initial point of the orbit lies in zone $\mathcal{Z}^{(n)}(l/m)=M^{-n}\mathcal{Z}^{(0)}(l/m)$, for some $n=0,\ldots,m-1$. Then, after $n$ iterations, it will lie in the principal zone $\mathcal{Z}^{(0)}(l/m)$. If it does not lie in an exiting turnstile lobe, it will visit again the $m$ zones of resonance $l/m$, returning to $\mathcal{Z}^{(0)}(l/m)$ after $m$ iterations. If, on the other hand, it lies in an exiting turnstile lobe, more precisely in some TO $\mathcal{O}(l/m\rightarrow l'/m')$ (see [22]), it will escape to zone $\mathcal{Z}^{(m'-1)}(l'/m')$ of resonance $l'/m'$, where it will perform at least a finite number of rotations (of $m'$ iterations each) before escaping to another resonance. Thus, a general orbit is a sequence of quasiregular segments, each lying in some resonance $l_r/m_r$, $-\infty<r<\infty$, and having a length of $q_r m_r$ iterations, where $q_r$ is the number of rotations performed in $l_r/m_r$ or number of successive visits of $l_r/m_r$. We denote this quasiregular sequence by $\tau=\ldots,(l_r/m_r)_{q_r},(l_{r+1}/m_{r+1})_{q_{r+1}},\ldots$, and say that the orbit is of *type* $\tau$ [8,9,20]. This is a considerable extension of the concept of Birkhoff type $(l,m)$ or $l/m$ of a PO [10,19]. In general, there are infinitely many orbits of given type $\tau$, forming a set $\mathcal{C}_\tau$. In some cases [7,8], $\mathcal{C}_\tau$ can be rigorously shown to be a fractal set with exactly calculable fractal properties.

## III. TYPE SPECIFICATION OF STABILITY ISLANDS

In this section, we consider the type specification of PO's for maps (1) [23] and show that it can be extended in a natural way to general stability islands. A PO of period $s$ for maps (1) is generally defined by $x_s=x_0$, $p_s=p_0+2\pi w$, where $w$ is an integer, generally nonzero; for $w\neq 0$, the PO is an "accelerator mode." In fact, this definition reduces to the usual one, $x_s=x_0$, $p_s=p_0$, if Eq. (1) is taken modulo the torus $0\leqslant x,p<2\pi$ [this can be always done consistently since Eq. (1) is $2\pi$-periodic in $p$]. Clearly, a PO can visit only a finite number of resonances modulo this torus. Thus, on the cylinder, it will generally visit a set of, say, $d$ resonances $\{l_r/m_r\}_{r=1}^d$ and all the translations $\{l_r/m_r+b\overline{w}\}_{r=1}^d$ of this set in the $p$ direction, where $b$ takes all the integer values and $\overline{w}$ is some integer which will be related to $w$ below. Therefore, the type $\tau$ of the PO must be essentially the repetition of some "block" $\Gamma$,

$$\tau=\ \ldots,\Gamma(-\overline{w}),\Gamma(0),\Gamma(\overline{w}),\Gamma(2\overline{w}),\ \ldots, \tag{2}$$

where

$$\Gamma(b\overline{w}) = (l_1/m_1+b\overline{w})_{q_1},\ \ldots,(l_d/m_d+b\overline{w})_{q_d} \tag{3}$$

and $q_r$ is the number of rotations performed in resonance $l_r/m_r+b\overline{w}$. Now, if the periodic cycle of the PO is completed exactly after visiting one block, then $w=\overline{w}$ and $s=\overline{s}$, where

$$\overline{s}=\sum_{r=1}^{d} q_r m_r \tag{4}$$

is the basic period. Generally, however, the periodic cycle is completed only after visiting more than one block—say, $c$ blocks. Then $w=c\overline{w}$ and $s=c\overline{s}$. The type of the PO will be thus specified by $(\Gamma,\overline{w},c)$, where $\Gamma$ stands, e.g., for $\Gamma(0)$.

Let us now consider a *stable* PO, such that each of its $s$ points is the "center" of an island in a chain of $s$ islands. In the simplest case, all the PO points lie within one resonance $l/m$ (outside the exiting turnstile lobes), so that $\Gamma(0)=(l/m)_q$ and $\overline{w}=0$ in Eqs. (2) and (3). Clearly, the type $(\Gamma,0,c)$ in this case is the same as $(\Gamma',0,cq)$, where $\Gamma'=(l/m)_1$, so that we can assume that $q=1$. The PO performs precisely $cl$ rotations in one period of $s=cm$ iterations—i.e., $x_{cm}=x_0+2\pi cl$ (no mod $2\pi$ taken). Since the resonance boundaries are stable and unstable manifolds which cannot cross an island, all the islands in the corresponding chain must lie within the resonance, outside the exiting turnstile lobes, like the PO points. One can therefore define the type of this chain (a "resonance" island chain) to be the same as that of its central PO.

The repetition index $c$ can be related to the concept of "class" of a PO [10], which we now recall. In each resonance $l/m$, there exists an elliptic or, for large parameter $K$, hyperbolic-with-reflection PO having period $m$ and the order-preserving property (defined in Sec. II) [4]. This is a "class-0" PO. A PO which rotates under the map $M^m$ around a point of the class-0 PO is a class-1 PO; we denote by $c_1$ the period of this PO under $M^m$. In general, a class-$j$ PO ($j>0$) rotates with period $c_j$ under the map $M^{\overline{c}m}$ ($\overline{c}=c_0c_1c_2\cdots c_{j-1}$, $c_0=1$) around a PO point of class $j-1$ and has precisely $c=\overline{c}c_j$ points in each zone of resonance $l/m$. Stable class-$j$ PO's are generally the "center" of corresponding class-$j$ island chains which form, for all $j$, an "islands-around-islands" hierarchy within a resonance $l/m$. As examples, Fig. 2 shows island chains of class 0 in resonances 1/3 and 1/2, of class 1 in resonances 1/3, 1/2, and 3/4, and of class 2 in resonance 1/2.

In the case that the stable PO visits more than one resonance—i.e., $d>1$ and/or $\overline{w}\neq 0$—the last PO point in a segment $(l_r/m_r+b\overline{w})_{q_r}$ of $\Gamma(b\overline{w})$ necessarily lies in the TO $\mathcal{O}(l_r/m_r+b\overline{w}\to l'/m')$, where $l'/m'=l_{r+1}/m_{r+1}+b\overline{w}$ for $r<d$ and $l'/m'=l_1/m_1+(b+1)\overline{w}$ for $r=d$. The island containing this point is clearly a "tangle" island [18], since the TO is part of an exiting turnstile lobe of resonance $l_r/m_r+b\overline{w}$. Actually, the tangle island must lie *entirely* within the TO. This is because the TO is separated from the rest of the exiting turnstile lobe by stable or unstable manifolds which would cross the tangle island if only part of this island lies in the TO. The islands associated with the other points in the segment $(l_r/m_r+b\overline{w})_{q_r}$ must lie entirely within resonance zones, outside the exiting turnstile lobes, like resonance islands. Thus, the entire island chain can be again characterized by a well-defined type, that of its central PO. For given type $(\Gamma,\overline{w},c)$, there are $cq_r$ islands in each zone of resonance $l_r/m_r+b\overline{w}$; in the principal zone $\mathcal{Z}^{(0)}$, $c$ of these islands lie in the TO.

As an example, we consider stable accelerator-mode PO's of the standard map [11]. The windows of the parameter $K$ for which these PO's exist in the case of $s=1$ (fixed points) can be easily determined [11]:

$$2\pi|w|<K<\sqrt{(2\pi w)^2+16}. \tag{5}$$

Such a fixed point is the center of an AI. Since $s=1$, it follows from $s=c\overline{s}$ and Eq. (4) that $d=q_1=m_1=c=1$, and one can choose $l_1/m_1=0/1$. Thus, the AI visits only main (first-order) resonances and its type is $\tau=\big((0/1)_1,w,1\big)$. Figures 1, 3, and 4 show the case of $w=1$ for $K=6.4717$. It is clear that the AI, which is a tangle island [18], indeed lies entirely within the TO of resonances 0/1 and 1/1. For general $w$, this is the TO of 0/1 and $w/1$. We remark that this TO starts to emerge for values of $K$ much smaller than those given by Eq. (5)—i.e., $K\approx 2(|w|-1)$ for large $|w|$. The last result can be easily derived from the conditions of TO for the sawtooth map [7], which approximates well the standard map for large $K$.

Figure 4 shows a class-1 chain of five islands surrounding the $s=1$ AI. For $K\approx 6.476\,939$, this chain appears to be the beginning of a self-similar islands-around-islands hierarchy

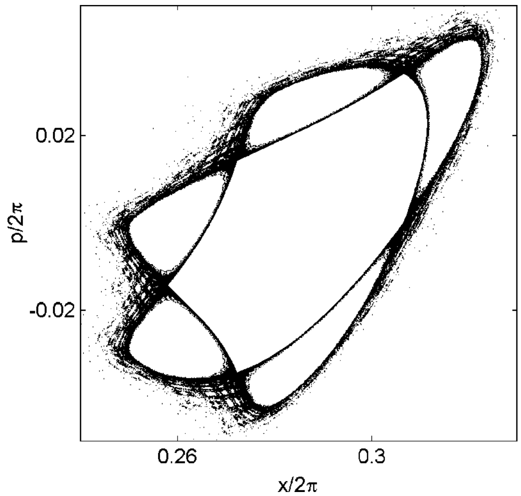


FIG. 4. Long chaotic orbit sticking around the AI that lies in the turnstile overlap (TO) $O_D$ shown in Fig. 3 (see more details in the text).

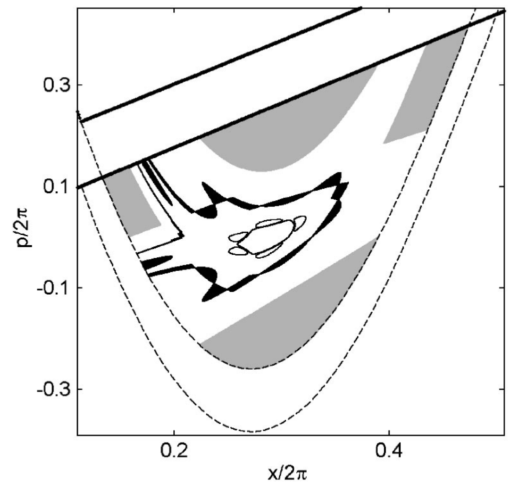


FIG. 5. Magnification of the TO $O_D$ in Fig. 3, showing the "trapped" sets $\mathcal{C}_1$ (grey regions) and $\mathcal{C}_5$ (black regions). These sets were calculated using the method mentioned in the caption of Fig. 2, starting from a grid of initial conditions covering the TO and having a resolution of $\Delta x/2\pi=\Delta p/2\pi=10^{-4}$. The set $\mathcal{C}_1$ coincides with $\mathcal{C}_1^{(0)}$ (see definition of $\mathcal{C}_t^{(0)}$ in the text) and appears to be indeed the first stage in the construction of a horseshoe, in consistency with relation (6).

with 11 islands in each class of order $j>1$ [13]. This hierarchy may then be specified by the general type $\tau=\boldsymbol{(}(0/1)_1,1,c\boldsymbol{)}$, where $c=5\times 11^{j-1}$.

## IV. DEFINITION OF CHAOTIC STICKINESS

We now show that the type specification of stability islands allows us to introduce in a natural way a precise generalized definition of chaotic stickiness. We first note that the type of a chaotic orbit sticking sufficiently close to the boundary of an island must coincide with the type of the island during the stickiness process. However, this coincidence of the types may also occur if the chaotic orbit is *not* "very" close to the island boundary: It expresses the fact that the chaotic orbit follows the itinerary of the island, specified by the type on the rotational level. This observation is at the basis of our definition: We say that a chaotic orbit of type $\tau_c$ "sticks" to an island chain of type $\tau=(\Gamma,\overline{w},c)$ if $\tau_c$ coincides with $\tau$ during a time interval of, say, $N$ iterations. This means that $\tau_c$ and $\tau$ have a common segment of $N$ resonance zones. It is easy to see that according to this definition the chaotic orbit sticks simultaneously to the island chains of type $\tau=(\Gamma,\overline{w},c)$ for all admissible values of $c$; the set of chains with $c>1$ will include, e.g., islands-around-islands hierarchies near the boundary of a class-0 ($c=1$) island (see previous section). One expects that if strong trapping occurs in a narrow "sticky layer" surrounding this boundary and adjacent to it, most chaotic orbits of type $\tau_c$ will approach this layer as $N\rightarrow\infty$.

To study in some detail first aspects of stickiness based on the definition above, let us restrict ourselves, for simplicity, to the important case of an AI with period $s=1$ and type $\tau=\boldsymbol{(}(0/1)_1,w,1\boldsymbol{)}$ (see the example in the previous section). We denote by $\mathcal{O}$ the TO of $0/1$ and $w/1$ in which this AI lies and by $\overline{M}$ the map (1) taken modulo the basic torus $0\leqslant x$, $p<2\pi$. Consider now all the chaotic orbits whose type $\tau_c$ coincides with $\tau$ in some time interval $n=n_1,\ldots,n_2$ ($n_2\neq n_1$) but differs from $\tau$ at times $n=n_1-1$ and $n=n_2+1$. Thus, $\tau$ and $\tau_c$ have a common segment of $N=n_2-n_1+1$ resonance zones, given by $(n_1w/1)_1,\ldots,(n_2w/1)_1$, so that the chaotic orbit "*accelerates* together" with the AI in the time interval above. Under the map $\overline{M}$, the orbit will lie in $\mathcal{O}$ for $n=n_1,\ldots,n_2-1$ but *outside* $\mathcal{O}$ for $n=n_1-1$ and $n=n_2$ (otherwise, $\tau$ and $\tau_c$ will coincide also at times $n=n_1-1$ and/or $n=n_2+1$). The segment of the orbit in $\mathcal{O}$ will therefore consist of $N-1$ points. We denote by $t_+$ ($t_-$) the forward (backward) exit time of any of these points from $\mathcal{O}$ under $\overline{M}$. It is easy to see that the *transit time* $t$, defined by [24] $t=t_++t_--1$, is equal to the length of the segment, $t=N-1$. The set of points in $\mathcal{O}$ having a given transit time $t$ will be denoted by $\mathcal{C}_t$. One can partition $\mathcal{O}$ into the sets $\mathcal{C}_t$, $\mathcal{O}=\cup_{t=1}^{\infty}\mathcal{C}_t$.

As an example, we consider again the AI of the standard map for $K=6.4717$ and $w=1$. Figure 4 shows a chaotic orbit sticking to this AI for a long time interval of $N=4\,563\,191$ iterations; i.e., the orbit lies in the main resonance $n/1$ for times $n$ in this interval. To determine the resonance in which the orbit lies at given time $n$, we use, as in Fig. 2, the efficient method introduced in Ref. [9], which avoids completely the problem of finding the resonance boundaries. Using this method, we found that the forward exit time of the initial ($n=0$) point of the orbit above from the TO under $\overline{M}$ is $t_+=3\,591\,053$ since $n=t_++1$ is the first time at which the orbit is not in resonance $n/1$ (but rather in $n+1/5$); then, $t_-=N-t_+$. The method was also used to calculate accurately the sets $\mathcal{C}_t$ for moderate values of $t$, starting from a large grid of initial conditions covering uniformly the TO. The results are shown in Figs. 5 and 6. We can see from Fig. 6 that as $t$ is increased $\mathcal{C}_t$ becomes highly concentrated on an "annulus" surrounding the AI boundary and approaching it. For $t=99$ [Fig. 6(c)] and $t=499$ [Fig. 6(d)], $\mathcal{C}_t$ already "wraps around"

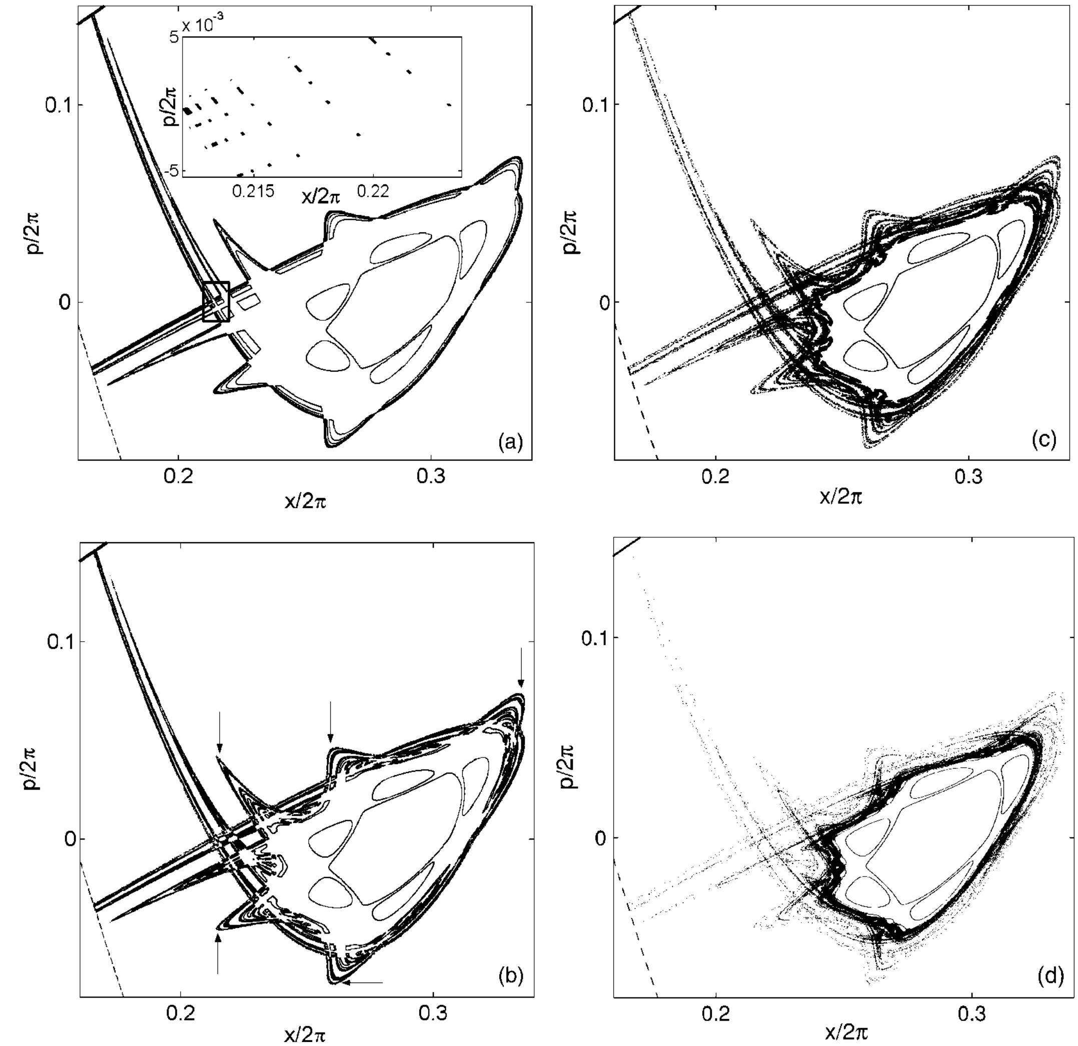


FIG. 6. Trapped sets $\mathcal{C}_t$ in the TO $O_D$ of Fig. 3: (a) $t=19$, (b) $t=29$, (c) $t=99$, and (d) $t=499$. Plots (a)–(c) were produced starting from the grid of initial conditions used in Fig. 5. In plot (d), a grid of higher resolution, $\Delta x/2\pi=\Delta p/2\pi=5\times10^{-5}$, was used. The inset in (a) shows a small portion of the set $\mathcal{C}_{19}^{(0)}$, lying within the rectangular region indicated. This set appears to be a high-order approximation of a horseshoe.

some island chains near the AI boundary. The structure of $\mathcal{C}_t$ becomes more intricate due to the development of new homoclinic intersections and oscillations. Most prominent oscillations are the five protuberances indicated by arrows in Fig. 6(b), which follow faithfully the shape of the five-island chain surrounding the AI. Interesting features of the homoclinic structure of $\mathcal{C}_t$ can be exhibited more clearly by looking, for $t$ odd, at the subset $\mathcal{C}_t^{(0)}$ of $\mathcal{C}_t$ consisting of all the points with $t_+=t_-=(t+1)/2$. It is easy to see that the set $\mathcal{C}_t^{(0)}$ satisfies the relation

$$\mathcal{C}_t^{(0)} \subseteq \bigcap_{n=-t_++1}^{t_+-1} \bar{M}^n\mathcal{O} - \bigcap_{n=-t_+}^{t_+} \bar{M}^n\mathcal{O}. \quad (6)$$

Since the TO $\mathcal{O}$ is a region bounded by stable and unstable manifolds, one expects from the form of the right-hand side of relation (6) that the structure of $\mathcal{C}_t^{(0)}$ should approximately resemble that of a horseshoe. This is shown in Fig. 5 for $t=1$ ($\mathcal{C}_1^{(0)}=\mathcal{C}_1$) and in the inset of Fig. 6(a) for $t=19$. A possible concentration of $\mathcal{C}_t^{(0)}$ around the islands boundaries as $t\to\infty$ is consistent with relation (6) and the fact that the set of all islands in $\mathcal{O}$ is obviously contained in $\bigcap_{n=-\infty}^{\infty}\bar{M}^n\mathcal{O}$.

We denote by $k_t$ the number of segments of length (transit time) $t$ having initial conditions on a large grid covering uniformly the TO; the total number of points in $\mathcal{C}_t$ is then $tk_t$. The quantity $k_t$ corresponds to the "trapping statistics" first studied by Karney [1] in connection with the stickiness problem in the Hénon map. Figure 7 shows a log-log plot of $k_t$ in the time interval $1\leq t\leq 10^3$ for the example above. We see that as $t$ is varied $k_t$ exhibits oscillations, which appear also for small $t$ in the main case studied in Ref. [1] [see Fig. 6(a) there]. In our case, the dynamical origin of these oscillations can be easily understood: they are due to the birth and development of new homoclinic structures in $\mathcal{C}_t$ as $t$ is increased; compare, e.g., Fig. 6(b) ($t=29$, $k_t=50\,909$) with Fig. 6(a) ($t=19$, $k_t=11\,747$). On average, $k_t$ clearly decays as a power law, $k_t\propto t^{-\alpha}$, $\alpha\approx 1.61$. This decay cannot continue for arbitrarily large $t$ since this will lead to a non-normalizable

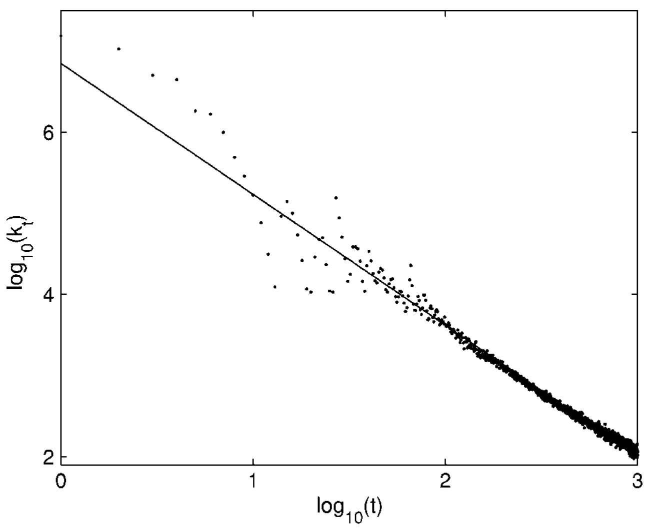


FIG. 7. Log-log plot of the "trapping statistics" $k_t$ in the TO $O_D$ of Fig. 3. The results were produced by starting, for all $t$, from the high-resolution grid used in Fig. 6(d). The linear fit to the data (solid line) has slope $\approx -1.61$.

function $tk_t$ for the number of points in $\mathcal{C}_t$. An asymptotic power-law decay of $k_t$ must feature an exponent $\alpha > 2$. The time interval considered thus belongs to a nonasymptotic time regime. A transition from the decay in Fig. 7 to a faster decay for large values of $t > 10^3$ could not be observed due to limitations in our available computational resources. The accuracy of the results in Figs. 6 and 7 was carefully checked by using a variety of different grids for the initial conditions in the TO.

## V. DISCUSSION AND CONCLUSIONS

We now discuss some of the main results above. According to a well-known phenomenological scenario [11,15], the superdiffusion of a chaotic ensemble, $\langle p_n^2 \rangle \propto n^{\mu}$ with $1 < \mu < 2$, is due to the long-time trapping of the chaotic orbits in a narrow "sticky layer" surrounding the boundary of an AI and adjacent to it (such as the sticky region in Fig. 4). During the trapping time, an orbit accelerates together with the AI and, after it leaves the layer, it enters the "chaotic sea" where it performs normal diffusion. A basic question concerns a precise and physically significant identification of the sticky layer—i.e., precisely which part of the chaotic region accelerates with the AI for at least some finite number of iterations? The results in the previous section provide an answer to this question. An orbit accelerates with the AI in some time interval if and only if it "sticks" to the AI according to the proposed definition of stickiness. Initial conditions for all the sticking orbits form *precisely* the TO region containing the AI. Thus, a physically significant sticky layer can be identified as the *chaotic component of the TO*. This is separated from the rest of the chaotic region (the "chaotic sea" which does *not* accelerate) by sharp boundaries—i.e., pieces of stable and unstable manifolds.

This identification of the sticky layer provides its natural *extension* much beyond a narrow strip adjacent to the AI boundary where the sticking time $t$ is usually quite long. The TO can be fully partitioned into sticky "sublayers" $\mathcal{C}_t$, where $\mathcal{C}_t$, $t \geqslant 1$, consists of all orbit segments having precisely length $t$ in the TO—i.e., segments accelerating with the AI for precisely $t$ iterations. As $t$ is increased, $\mathcal{C}_t$ gradually approaches the AI boundary (see Fig. 6). The consideration of all sticking times is necessary for studying the superdiffusion and other stickiness-related phenomena in a nonasymptotic time regime (which can be *very long* in practice) and for understanding how precisely these phenomena set into their asymptotic behavior (assuming it exists). It is also necessary for investigating the fingerprints of classical superdiffusion in the quantized version of the system, where dynamical localization implies a finite maximal spread of a wave packet, reached in a finite time $t$ [25].

A first study of a nonasymptotic time regime was performed in the previous section. The accurate results in Figs. 6 and 7 show that the usual features attributed to "stickiness" in the asymptotic time limit $t \to \infty$ are exhibited by $\mathcal{C}_t$ already for $t < 10^3$ (with $\mathcal{C}_t$ still *far* from being adjacent to the AI boundary): A relatively high concentration of orbit points on a subregion of $\mathcal{C}_t$ [see Figs. 6(c) and 6(d)] and a clear power-law decay of the trapping statistics $k_t$ (see Fig. 7).

These results cannot be reproduced by any empirical approach in which the trapping near an island is studied by enclosing the island in an *arbitrary* region, a "box" (see, e.g., Ref. [1]). As one can see from Figs. 5 and 6, *no* such region, except of the TO, can completely contain the trapped accelerating sets $\mathcal{C}_t$ for *all t* if it will not also contain nonrelevant parts of the chaotic sea which do not accelerate but will be nevertheless considered as "trapped." In general, all the sets $\mathcal{C}_t$ sticking to a given island chain are determined from the ensemble of chaotic orbits whose type (sequence of resonances visited) coincides with that of the island chain in some time interval. This ensemble is easily found using the efficient method developed in Ref. [9] which completely avoids the problem of calculating the resonance boundaries. Thus, the dynamically well-defined and practically applicable approach to stickiness introduced in this paper can form the basis for a most systematic study of anomalous chaotic transport and related phenomena.

[1] C. F. F. Karney, Physica D **8**, 360 (1983).
[2] R. S. MacKay, J. D. Meiss, and I. C. Percival, Physica D **13**, 55 (1984).
[3] J. D. Meiss and E. Ott, Physica D **20**, 387 (1986).
[4] R. S. MacKay, J. D. Meiss, and I. C. Percival, Physica D **27**, 1 (1987), and references therein.
[5] Q. Chen, Phys. Lett. A **123**, 444 (1987).
[6] I. Dana, N. W. Murray, and I. C. Percival, Phys. Rev. Lett. **62**,

233 (1989).
[7] Q. Chen, I. Dana, J. D. Meiss, N. W. Murray, and I. C. Percival, Physica D **46**, 217 (1990).
[8] I. Dana, Phys. Rev. Lett. **64**, 2339 (1990).
[9] I. Dana, Phys. Rev. Lett. **70**, 2387 (1993), and references therein.
[10] J. D. Meiss, Rev. Mod. Phys. **64**, 795 (1992), and references therein.
[11] R. Ishizaki, T. Horita, T. Kobayashi, and H. Mori, Prog. Theor. Phys. **85**, 1013 (1991).
[12] G. M. Zaslavsky, M. Edelman, and B. A. Niyazov, Chaos **7**, 159 (1997).
[13] S. Benkadda, S. Kassibrakis, R. White, and G. Zaslavsky, Phys. Rev. E **55**, 4909 (1997).
[14] R. B. White, S. Benkadda, S. Kassibrakis, and G. M. Zaslavsky, Chaos **8**, 757 (1998).
[15] G. M. Zaslavsky and M. Edelman, Chaos **10**, 135 (2000).
[16] G. M. Zaslavsky, Phys. Rep. **371**, 461 (2002), and references therein.
[17] I. Dana, Phys. Rev. E **69**, 016212 (2004).
[18] V. Rom-Kedar and G. Zaslavsky, Chaos **9**, 697 (1999), and references therein.
[19] Ordered or monotone PO's are also known as *Birkhoff* PO's; see, e.g., Y. Yamaguchi and K. Tanikawa, Prog. Theor. Phys. **111**, 689 (2004).
[20] In previous works [4–9], a resonance was denoted by $(l,m)$ and a similar notation was used in the expression of the type $\tau$ of a general orbit [8,9]. For simplicity, however, we use here the winding-number notation $l/m$.
[21] For $K \leqslant K_c$, the resonances give a partition of any phase-space region bounded by two rotational tori but within which no such tori exist.
[22] The resonance partition implies that an exiting turnstile lobe of a resonance $l/m$ can be completely partitioned into the turnstile overlaps $\mathcal{O}(l/m \to l'/m')$ with all the other resonances. See, e.g., Refs. [6–8].
[23] The type specification of PO's, as presented here, is substantially different from that given in Ref. [8].
[24] J. D. Meiss, Chaos **7**, 139 (1997).
[25] A. Iomin, S. Fishman, and G. M. Zaslavsky, Phys. Rev. E **65**, 036215 (2002).